SLAC-PUB-17117

A Traveling-Wave Forward Coupler Design for A New Accelerating Mode in A Silicon Woodpile Accelerator

Ziran Wu, *Member, IEEE*, Chunghun Lee, Kent P. Wootton, Cho-Kuen Ng, Minghao Qi, *Member, IEEE*, and Robert Joel England

***Abstract*—Silicon woodpile photonic crystals provide a base structure that can be used to build a three-dimensional dielectric waveguide system for high-gradient laser driven acceleration. A new woodpile waveguide design that hosts a phase synchronous, centrally confined accelerating mode is proposed. Comparing with previously discovered silicon woodpile accelerating modes, this mode shows advantages in terms of better electron beam loading and higher achievable acceleration gradient. Several traveling-wave coupler design schemes developed for multi-cell RF cavity accelerators are adapted to the woodpile power coupler design for this new accelerating mode. Design of a forward coupled, highly efficient silicon woodpile accelerator is achieved. Simulation shows high efficiency of over 75% of the drive laser power coupled to this fundamental accelerating mode, with less than 15% backward wave scattering. The estimated acceleration gradient, when the coupler structure is driven at the damage threshold fluence of silicon at its operating 1.506 μm wavelength, can reach 185 MV/m. A 17-layer woodpile waveguide structure was successfully fabricated, and the measured bandgap is in excellent agreement with simulation.**

***Index Terms*—Electron accelerators, optical waveguides, photonic crystals, silicon devices, couplers.**

I. Introduction

LASER driven optical structures for charged particle acceleration have been an emerging research field in recent years, showing great potential in reaching ~ GeV/m level acceleration gradients [1-6] and orders of magnitude footprint and cost reduction [1, 5, 6] when compared to conventional RF accelerators. In addition, non-cryogenic operation of these optical accelerator structures at kHz to MHz repetition rate, as well as sub-fs electronic and photonic bunch structures could enable ultrafast dynamics studies and boost average output power when they are used as radiation generation devices. Experimental demonstrations of this concept have been focused on so-called "phase-reset" dielectric structures in the near-infrared spectrum range, such as fused silica gratings [2, 3] and silicon pillar arrays [4]. There the drive laser is transversely incident on the accelerator structures with its electric field polarized along the electron's direction of motion, and the structures provide a modulated phase front of the laser field based on optical path differences, so that net acceleration of the electron velocity can be achieved [1]. Gradients up to 300 MV/m have been observed in these experiments, an order of magnitude higher than typical operating gradients in conventional metallic structures at radio frequencies [2-4].

Another approach of laser driven near-field structure acceleration is the employment of optical waveguides. Given the practical difficulty in fabricating metallic waveguides of optical-wavelength dimensions, as well as the large Ohmic loss and the lower breakdown thresholds of metal surfaces under strong laser fluence [2], dielectric materials are a more suitable choice for making these optical waveguides. In this application as a particle accelerator, it is necessary to provide a material-free hollow core waveguide for charged particles to traverse. Therefore, photonic crystal based hollow-core waveguides such as 1-D Bragg fiber, 2-D photonic bandgap (PBG) fiber, and 3-D photonic bandgap waveguides [7], become ideal candidates to build dielectric laser accelerators (DLAs).

To serve the purpose of particle acceleration, a waveguide structure must support a transverse-magnetic (TM) like mode, with the major electric field component polarized along the longitudinal direction of the waveguide. Another character in demand of this accelerating mode is phase synchronicity, i.e. its phase velocity equals the speed of light so that relativistic particles could be driven by the laser's electromagnetic (EM) wave at a constant optical phase for continuous acceleration. Previous theoretical explorations have found several such modes in dielectric photonic crystal waveguides [5, 6, 8, 9], and their performances as fundamental accelerating modes have been evaluated. An accelerating optical waveguide hosts a transversely closed environment for laser and charged particle interaction with less interference from the environment, as well

Manuscript is submitted for review on June 1st, 2015. This work is supported by U.S. Department of Energy under Grants DE-AC02-76SF00515, DE-FG02-13ER41970 and by DARPA Grant N66001-11-1-4199.

Z. Wu is with SLAC National Accelerator Laboratory, Menlo Park, CA 94025 USA (e-mail: wzr@slac.stanford.edu).

C. H. Lee is with Purdue University, West Lafayette, IN 47907 USA (e-mail: lee.chunghun@gmail.com).

K. P. Wootton is with SLAC National Accelerator Laboratory, Menlo Park, CA 94025 USA (e-mail: wootton@slac.stanford.edu).

C. K. Ng is with SLAC National Accelerator Laboratory, Menlo Park, CA 94025 USA (e-mail: cho@slac.stanford.edu).

M. H. Qi is with Purdue University, West Lafayette, IN 47907 USA (e-mail: mqi@purdue.edu).

R. J. England is with SLAC National Accelerator Laboratory, Menlo Park, CA 94025 USA (e-mail: england@slac.stanford.edu).

This material is based upon work supported by the U.S. Department of Energy, Office of Science, under Contract No. DE-AC02-76SF00515.

as electromagnetic energy confinement and co-propagation along its core with strong spatial overlap with the particles to enhance the interaction. However, the enclosed near-field structure implies challenge in coupling external laser power to the waveguide, especially when the target is a TM-like accelerating mode [9, 10].

This work is focused on a three-dimensional dielectric PBG waveguide based on the so-called "woodpile" photonic crystal structure (WPS). Several accelerating modes have been proposed with different woodpile waveguide designs [6, 9] so far. Individual rods in the woodpile structure discretize the spatial dielectric distribution; therefore offering several degrees of freedom for mode selection [9] and allowing various coupling and deflection/focusing elements [11]. The choice of silicon as the build dielectric material is intended to be well-suited to standard wafer MEMS photolithography processes, potentially leading to on-chip particle accelerators.

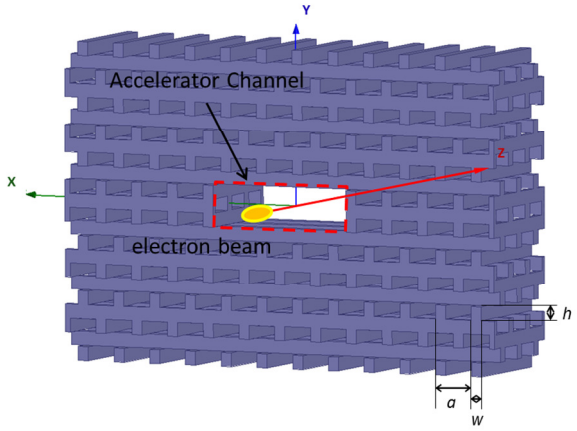

Figure 1. Schematic of a silicon woodpile accelerating waveguide.

A woodpile photonic crystal structure is an arrangement of high-index dielectric scatterers in a low-index background material (e.g. air), following a woodpile formation. The schematic in Fig. 1 shows a typical silicon woodpile waveguide. The base lattice consists of rectangular silicon rods stacked layer-by-layer, whose collective scattering of light exhibits a three-dimensional photonic bandgap, such that no light in the PBG frequency range can propagate in the lattice. A defect channel with a rectangular aperture can be opened in the lattice to form a waveguide, as illustrated by the red dashed line in Fig. 1. The lattice and the waveguide channel possess mirror symmetry about the XZ plane, therefore permitting a symmetric monopole mode in the waveguide for acceleration.

Because of the photonic bandgap, a traveling waveguide mode has its energy tightly confined in the accelerator channel, co-propagating with the electron bunch (yellow ellipsoid, Fig. 1) along the Z direction. The woodpile lattice dimensions w, h, and a are silicon rod width, silicon rod height, and rod spacing within each layer, respectively as marked in Fig. 1. The waveguide channel shown here is $3h$ tall and $4a$-w wide along its two transverse directions, which hosts an ideal accelerating mode as will be shown in Section II. A nominal set of dimensions have been used, with w = 158 nm, h = 200 nm, and a = 565 nm. Such dimensions result in a silicon woodpile lattice with photonic bandgap centered at 1.55 μm wavelength, with about 16.4% bandgap width to center frequency ratio.

After a fundamental accelerating mode is found, the next critical component is a coupler that delivers external drive laser power, ideally exclusively to this mode. This power coupler should be aimed to be highly efficient, compact, and easy to fabricate. Recently, a side coupler design very much in analogy with TE-to-TM waveguide couplers in microwave accelerators has been proposed [9]. Therein the side coupler guide is formed by a silicon-on-insulator (SOI) waveguide, consisting of a silicon slab sitting atop a lower-refractive-index substrate, employing total internal reflection of silicon to confine light. Although shown with almost perfect efficiency in simulation, the coupler design of Ref. [9] is essentially not complete because it uses symmetric boundary conditions to terminate the longitudinal ends of the accelerating waveguide. The result is that laser power is evenly split into both forward and backward directions after the coupler. It is the main motivation of this work to advance the design to a fully forward coupler. This coupler we present in Section III is designed for a new woodpile accelerating mode, as described in Section II, which exhibits several improvements over other accelerating modes reported. As a demonstration, 17-layer and 9-layer woodpile accelerator waveguide structures have been fabricated and are discussed in Section IV.

II. A New Accelerating Mode

Several accelerating waveguide designs based on silicon woodpile structures have been proposed before [6, 9]. The transverse profiles, phase and group velocities of the accelerating modes can be fine-tuned by adjusting the waveguide aperture size and the details at the channel wall. As an example, plotted in Fig. 2(a) is the vector electric field of a previously designed propagating TM mode, showing a large longitudinal electric field component for acceleration. Parameters of this accelerating mode and a coupler design to transfer laser power to this mode can be found in [9]. Instead of a straight rectangular aperture in the woodpile lattice as illustrated schematically in Fig. 1, the design in Fig. 2(a) has an attached silicon piece at the –X boundary of the waveguide wall towards the waveguide center (as the black arrow points out) to tune the dispersion curve of this mode down in frequency, so that to make it intersect the speed-of-light line for synchronous particle acceleration.

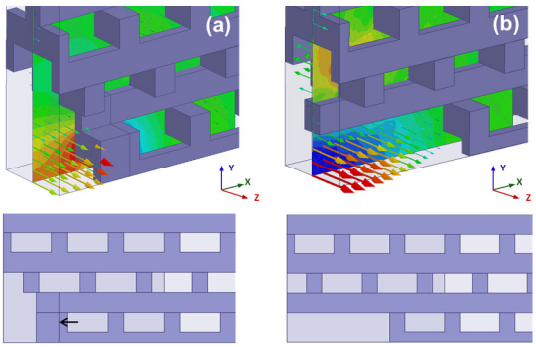

Figure 2. TM-like propagating modes of (a) a previously proposed [9] and (b) a newly designed woodpile waveguide, with their vector electric fields plotted.

Note that only one quarter of the full structure is modeled, with its front YZ plane and bottom ZX plane assigned to perfect magnetic boundaries to simulate TM accelerating modes. The bottom two figures show their cross sections in the XY plane, respectively, to better illustrate their waveguide apertures.

Although this prior design is a good candidate for laser acceleration and more than 95% power coupling to this mode has been achieved in simulation, it has a few disadvantages regarding its modal profile in the waveguide. As can be seen from its electric field profile in Fig. 2(a), the maximum of the field is located in the silicon at the waveguide wall along -X direction, leaving it prone to laser damage at this location. The transverse profile of the mode departs significantly from a Gaussian distribution, with the accelerating field at the core significantly lower than that near the silicon wall. In addition, this waveguide has a rather small transverse dimension of 1.175a width and 5h height, and therefore fewer electrons can pass through the aperture without hitting the silicon.

Here we propose a new woodpile waveguide geometry with an improved accelerating mode. The vector electric field of this mode is illustrated in Fig. 2(b). The new design has a full aperture dimensions of 4a-w by 3h, almost double the channel cross-section of the design in Ref. [9] given the nominal a, w, and h values aforementioned, resulting in greater electron transmission. Its longitudinal field distribution has the power concentrated along the waveguide center, which is better matched to an electron beam transverse profile of presumably Gaussian distribution. This profile is also advantageous to avoid laser damage to the dielectric, since the energy is mostly confined in the vacuum core.

The dispersion of this new accelerating mode and the profile of the longitudinal component of its electric field are presented in Fig. 3. Observing that the dispersion curve intersects with the speed-of-light line at 199.2 THz (1.506 μm wavelength), this mode will be phase synchronized with relativistic electrons when excited at this frequency. Near this operating frequency, this mode has a group velocity of 0.109c with c being the speed of light constant, which is also slightly higher than that of the prior design in Ref. 9. This results in less laser pulse "slippage" from the electron bunch as the mode propagates. However, this new accelerating mode still has a group velocity of only about 10% of the speed of light. This low group velocity implies the necessity of frequent injections of new drive laser pulses to the electrons, further demanding compact and easy to fabricate couplers [12]. The abscissa of Fig. 3 is defined as the phase advance per waveguide cell, instead of a continuous phase velocity. As will be further explained in Section III, this is due to the longitudinal periodic nature of a propagating woodpile waveguide mode exerted naturally by the periodic dielectric structure itself.

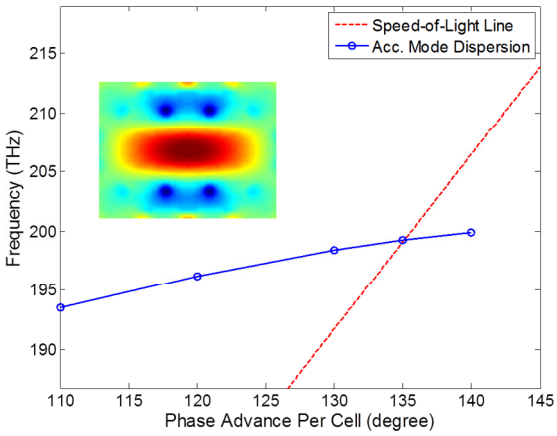

Figure 3. Dispersion curve of the new woodpile accelerating mode. Inset shows a full transverse colormap of its longitudinal electric field component.

III. Power Coupler Designs

The side coupler design of Ref. [9] is adapted to couple laser power into this new accelerating mode. The design utilizes a widened silicon rod perpendicular to the woodpile accelerating waveguide, extending into the vacuum core as a guide for the laser power. The side extrusion of the coupling guide provides minimum obstruction to the electron traverse channel, and this silicon coupling guide could potentially be monolithically fabricated with the woodpile waveguide.

Unlike two-dimensional waveguides such as SOI guides and solid-core optical fibers, a woodpile waveguide is periodically loaded in the longitudinal direction (as the waveguide direction) as a result of the three-dimensional layout of its photonic base lattice. Because of this periodic longitudinal variation, a transversely (cross-sectional) matched incident mode profile would not be sufficient to launch the propagating mode in the woodpile guide appropriately. Consequently, matching is needed also along the longitudinal propagation direction or else significant scattering loss would occur.

Two design schemes inherited from power coupler designs for disk loaded RF accelerator waveguides have been proposed and found applicable to silicon woodpile waveguides before [9]. The first scheme is a traveling-wave launch method for periodically loaded waveguides [13], which utilizes a discontinuity in the side coupler guide to introduce correct phasing to all the space harmonics needed for a traveling wave excitation. The second scheme serves to evaluate the quality of the traveling-wave launch and of whether the power is efficiently coupled to the targeted accelerating mode. This is done by calculating the normalized backward-wave-amplitude and the phase advance per cell along the woodpile waveguide [14]. Formulations and procedures of these two schemes are explained in details in Ref. [9]. Here they are directly implemented in designing a power coupler for this new woodpile accelerating mode.

A. *Back-to-Back Symmetric Setup*

A back-to-back symmetric coupler is first studied via finite element simulations [15]. The advantage of a back-to-back

setup is that it uses exactly the same input coupler as the output coupler, so that no reflection is caused by the mismatch if the setup contains only one input coupler and the waveguide output end is terminated by open space or imperfect absorbing boundaries. The disadvantage is that the setup uses symmetric boundary conditions at the entrance and exit of the accelerating waveguide: effectively the laser power coupled in is equally split between the forward and backward longitudinal directions. Figure 4 below illustrates the equivalent back-to-back waveguide model (dashed lines) of a symmetric model (solid lines) due to the application of symmetric boundary conditions, as well as the splitting of the laser power flow in the forward and backward directions (red arrows). The result is that only half of the total power coupled to the accelerating waveguide can be used to accelerate the forward traveling electron bunch along the +Z direction.

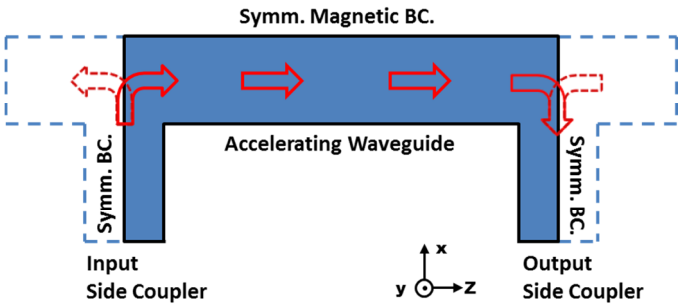

Figure 4. A schematic showing a back-to-back symmetric waveguide model (solid black lines), its input and output couplers, and the laser power flow (solid red arrows). The equivalent model due to the symmetric boundary conditions (BC.) applied in XY planes is illustrated in dashed blue lines, with effectively equally split laser power (dashed red arrows) at the coupling corners.

The layout in Fig. 5 illustrates a back-to-back side coupler design for the new woodpile accelerating mode. The model is a quarter-symmetric structure, with its front YZ plane and bottom ZX plane assigned to perfect magnetic boundaries to simulate TM-like accelerating modes. A pair of widened silicon rods, having a full width of 3.32w and height of h, act as input and output side power couplers at the beginning and end of the accelerating waveguide (as marked in Fig. 5). Because of the perfect electric boundary conditions assigned at the XY planes on the outer boundary of the model, a TE mode polarized in the Z direction is excited by the waveport assigned on the input coupler rod, highlighted by the light blue arrow in the layout. This TE mode then propagates into the accelerating waveguide along the +Z direction, after the TE mode to TM mode conversion at the coupling corner. After the accelerating waveguide section, the power is coupled out via the output coupler placed exactly in mirror symmetry with the input coupler.

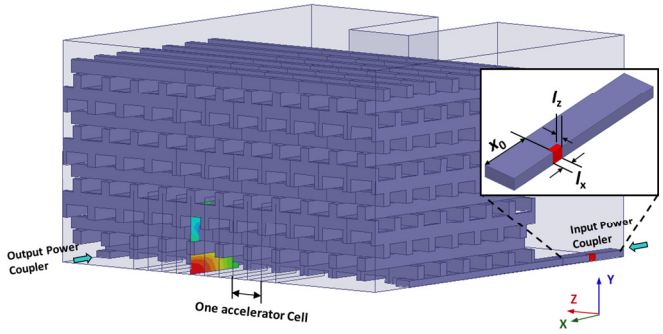

Figure 5. A symmetric back-to-back TE to TM mode coupler layout for a 9-cell woodpile accelerating waveguide. The inset image shows the launcher section of the silicon rod side coupler.

As described in Ref. [9], the traveling-wave launcher is built by perturbing the TE mode propagation in the side coupler silicon rods with an embedded element of perfect conductor, as illustrated in Fig. 5. The optimal complex reflection coefficient S_{22}^{m} of this mode launcher section (looking away from the woodpile structure) is determined by a multiple-cell simulation [13]. In the simulation, the number of woodpile accelerator cells is varied between the input and output coupler guides (Fig. 5, however without the launcher section), and S-parameters of the whole structure evaluated. As a fully matched coupler requires, a condition that with this launcher section, the reflection of the full structure at the input port needs to be zero must be satisfied. Therefore the magnitude and phase of the S_{22}^{m} of the launcher section are related as a function. Curves of this function corresponding to different numbers of accelerator cells then intersect at a common point, because a perfectly coupled traveling wave propagates identically in the woodpile waveguide regardless of the number of accelerator cells. This common point gives the desired S_{22}^{m} of the launcher section for a traveling-wave excitation, and for the case studied here this optimal value is 0.772 in magnitude and 166.8° in phase.

Optimization is achieved via tuning the dimensions of the embedded perfect conductor in the launcher silicon rod. The depth of the element along the Z direction (denoted as l_z in Fig. 5 (inset)) provides direct control to tune the magnitude of the S_{22}^{m}, whereas the distance between the PEC element and the front end of the launcher (denoted as x_0) determines its phase independently. The element length l_x along the X direction serves as a third parameter to fine tune the magnitude and phase. For a launcher section length of 1.5 µm and half-width of 262.5 nm, l_x = 133 nm, l_z = 74 nm, and x_0 = 0.709 µm yield the desired S_{22}^{m}.

Figure 5 presents the structure with optimized launch. The simulated total power transmission is 77%, with less than 10% normalized backward-wave-amplitude $|R|$ indicating a good traveling wave launch. The 23% energy loss is a combination of remnant backward wave and light scattering at the coupling corner. The launched longitudinal E-field profile, as plotted by the colormap on a transverse cut plane in the accelerating waveguide in Fig. 5, closely resembles the target accelerating mode in Fig. 3. The condition of phase synchronicity is also

met, with a nearly uniform phase velocity of 1.0037c along the woodpile waveguide section.

The sensitivity of the traveling-wave launch to dimensions and metal conductivities of the embedded scatting piece in the silicon coupler rod is studied. Copper, Chromium and Gold as commonly used metals in nano-fabrications are used as the materials of the scatterer, and they give negligible changes to the S-parameters of the mode launcher section. Therefore a metal scatter of conductivity as low as 7.7e6 Siemens/m would not affect the coupling quality. Also it is found via simulations that the coupling is more sensitive to the phase of the mode launcher S_{22}^{m} than its magnitude, which is directly controlled by the dimension x_0 of the scatterer. A 10° phase change in silicon at 1.506 μm design wavelength (free space) then correspond to 12 nm variation of x_0. As a fine-tune parameter affecting both the magnitude and phase of S_{22}^{m}, l_x shows about 15 nm variation range before the normalized backward-wave-amplitude increases to more than 20% and the total transmission of the coupled structure drops to 71.5%.

B. Forward-Propagating Mode Power Coupler

To design an input launch propagating power preferentially in the forward direction, the symmetry electric boundary conditions used on the XY termination planes of the back-to-back model in Fig. 5 need to be replaced by open boundaries, or continuation of the woodpile waveguide. In order to avoid laser power going into the backward direction (-Z) after the input coupler guide, a smaller woodpile waveguide with reduced height is designed as the termination. This lower-clearance waveguide exhibits a cut-off to the woodpile accelerating mode and thus prevents power propagation in the undesired direction, as is analogous to the cutoff beam pipes terminating conventional RF accelerators.

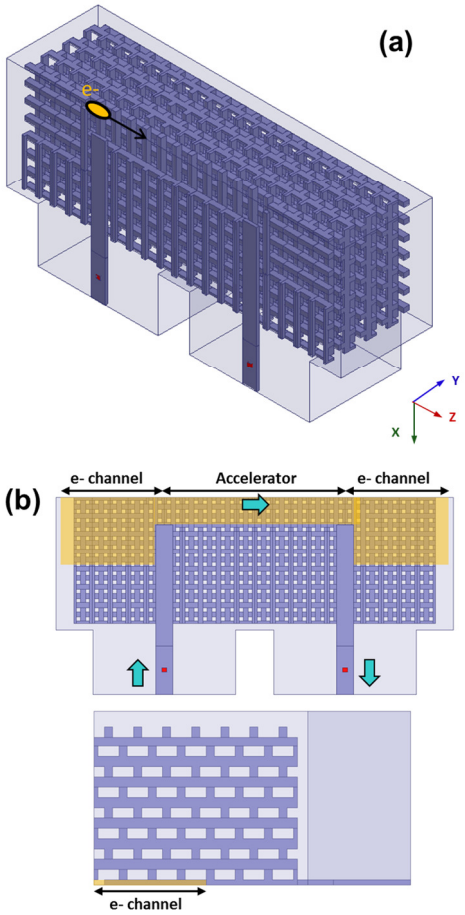

Figure 6. (a) The schematic of a fully forward coupled silicon woodpile accelerator, and (b) its bottom view and side view highlighting its open sections as the electron channel and the accelerating waveguide.

Figure 6(a) shows the schematic of a forward coupler design, with 9 accelerator cells in the woodpile accelerating waveguide section. The schematic presents one quarter of the mirror-symmetric full structure in its transverse XY plane, to better illustrate its woodpile waveguide structures. The accelerator waveguide section is identical to the back-to-back setup in Fig. 5.

This design additionally implements two cut-off waveguide sections at the forward and backward Z ends of the back-to-back symmetric model to confine the laser power propagation within the accelerator section. The cut-off waveguide has a full dimension of height h along the Y coordinate, and width $8a$-w along the X coordinate. It is found via eigenmode simulations [15] that this reduced height from the accelerating waveguide ($3h$) prevents the accelerating mode from leaking into the termination sections. This cut-off is mainly due to the reduced waveguide height, hence the cut-off waveguide width is made quite large to allow larger transverse aperture for the electron beam. Figure 6(b) presents views from the bottom and into the longitudinal direction, respectively, with the opening areas in the structure highlighted by light yellow shaded areas. The light-blue arrows again mark the direction of the laser power flow in the coupler structure.

Finite element simulations of the structure presented in Fig. 6 have demonstrated that the cut-off sections effectively prevent

the backward mode propagation, preferentially directing the energy from the input coupler guide into the accelerator section, and coupling it out via the output coupler guide.

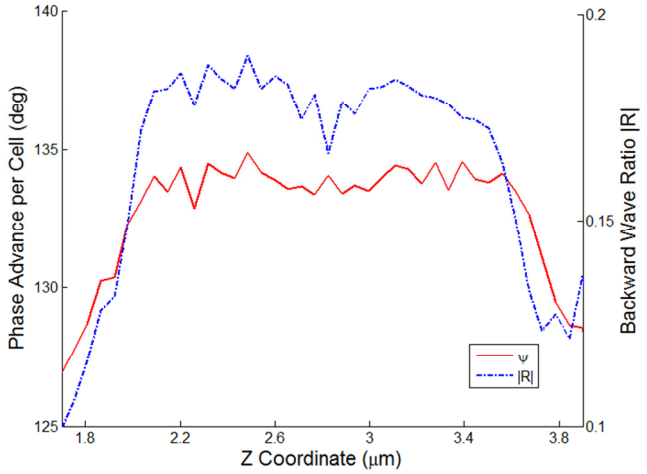

Figure 7. The phase advance per cell ψ and the normalized backward-wave amplitude $|R|$ of a 9-cell forward coupler structure. Transition regions where couplings are establishing are observed before ~ 2.1 μm and after ~ 3.6 μm in Z coordinate. The plateau region in the middle is about 2.7 woodpile accelerating cells long, with ~ 134° per-cell phase advance for phase synchronicity.

At its operation wavelength of 1.506 μm, the simulated total power reflection of this fully forward coupler is less than -22 dB, and its total power transmission is -1.21 dB. The excited electric field profile in the accelerating waveguide again replicates the targeted accelerating mode in Fig. 3 well. Plotted in Fig. 7 are the phase advance angle ψ per accelerator cell and the normalized backward-wave-amplitude $|R|$ along the accelerating waveguide. Both show relatively flat regions in the middle and transition regions of about 3 accelerator cells long at the input and output coupling corners, leaving an effective acceleration section of about 2.7 cells. The phase advance angle ψ per cell is about 134° (left ordinate), thus achieving the phase synchronous condition for a drive wavelength of 1.506 μm. The normalized backward-wave-amplitude $|R|$ is ~ 17.5% (right ordinate), suggesting a predominantly traveling-wave excitation.

Based on these simulations, a coupling efficiency of 75.7% to the forward-propagating accelerating mode is reached. This forward power coupler, although still a quarter-symmetric structure transversely, is a complete structure in its longitudinal direction and can be used as an individual accelerator unit of high efficiency.

IV. Fabrication

Although a 3-D silicon woodpile structure provides a true waveguide system in analogy to metallic waveguides, it is challenging to manufacture this complicated structure. The major challenge is to fabricate the 3-D structure with high yield and fast turn-around time, especially when the number of layers in the stacking direction is large. At least 6 layers of silicon rods are needed on top and bottom of the waveguide to sufficiently confine the laser energy. The waveguide opening is usually 3 to 5 layers tall, thus the full structure reaches 15-17 layers. Prior efforts have succeeded in making full structures using polymer 3D prototyping and silicon inversion methods but with significant lattice distortion near the waveguide defect, as well as 8 to 9 layer half-structures using standard photolithography [16, 17].

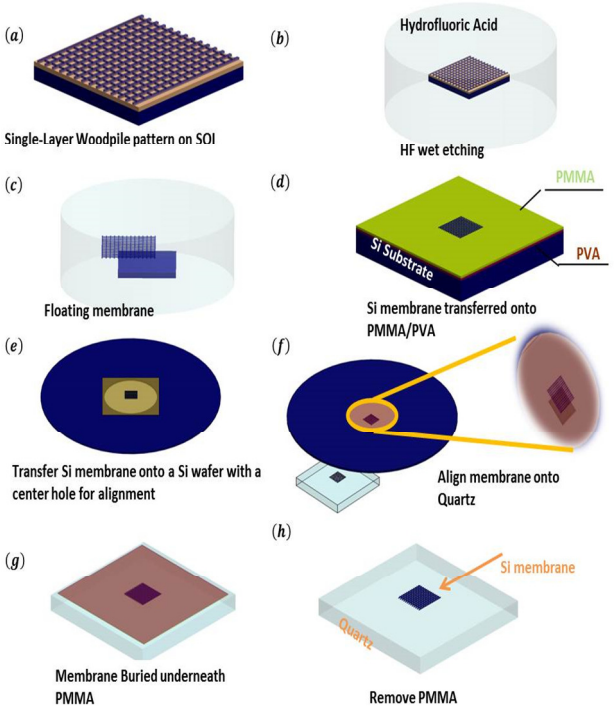

Figure 8. Membrane transfer processing: (a) A silicon-on-insulator piece (b) HF wet etching (c) Single pattern layer (d) Si membrane transfer (e) Transfer Si membrane on perforated substrate (f) Align Si membrane on pure Si substrate or Glass (g) Remove PMMA by Oxygen plasma (h) single transferred Si membrane and repeat above processing to stack a 17-layer woodpile structure.

Here a new approach to form woodpile waveguide structures has been implemented, by transferring and stacking pre-patterned, free-standing silicon membranes. This technique does not require high temperature processes, allows flexibility in the choice of materials, and makes prototyping of woodpile stacks of 10 to 20 layers feasible.

The flow chart of the overall fabrication process is depicted in Fig. 8. The woodpile pattern is first etched on the top layer of an SOI wafer, and then released from the substrate with HF wet etching. The released membrane is then transferred on top of a polymethyl methacrylate (PMMA) film, separated from a silicon substrate by a polyvinyl alcohol (PVA) film. Then the PMMA/PVA/woodpile film is again mounted on a handling silicon wafer with an opening at the center where the woodpile structure will be located. This handling wafer is flipped with the woodpile facing down, and then aligned and stacked onto a substrate with previously transferred woodpile layers. After dissolving the PMMA/PVA layers by oxygen plasma etching [18], more layers can be stacked by repeating this process.

To achieve high quality woodpile structures, this fabrication process requires high precision alignment of the stacked layers. The apparatus combines multi-axis nanometer piezo translation stages, an interferometer setup for transverse alignment, and

bonding apparatus. Using this new fabrication process and precise alignment and bonding stages, 9-layer and 17-layer woodpile waveguide structures have been successfully fabricated. Figure 9 illustrates SEM images of a fabricated 17-layer structure. This structure was fabricated before the new accelerating mode of the present work was identified; hence the fabricated waveguide is *a*-*w* wide and 5*h* tall corresponding to the prior design in Ref. [9]. The target wavelength is set to be around 3 μm considering the fabrication difficulty, the achievable feature sizes, and the drive laser source available. This results in a structure scaled about twice the dimensions of the simulation design. The drive wavelength of 3 μm would also be further away from the absorption band of silicon near 800 nm, therefore less dielectric material absorption loss. The final structure dimensions are 415 nm width (*w*), 494.75 nm height (*h*), and 1.18 μm rod periodicity (*a*), as measured from the zoomed-in SEM image of the fabricated sample in Fig. 9(b).

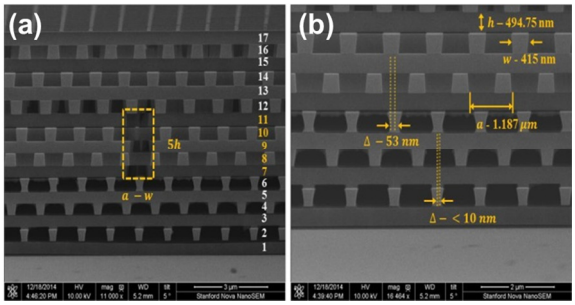

Figure 9. A 17-layer woodpile structure. The target wavelength is set to 3 μm and the waveguide was designed *a*-*w* wide and 5*h* tall, located between the 7th and 11th layers. The average misalignment of layers is about 53 nm.

As illustrated by the mesh pattern in Fig. 8(a), additional thin rods interlacing the woodpile lattice rods have been fabricated in each layer to protect the lattice rods from breaking during the membrane transfer and cleaning processes. These thin support rods have the same height as the lattice rods, and are about 100 nm wide. After assembly of the layers, these thin rods can be removed by silicon oxidation and vapor HF etching. The thin rod removal process has not yet been perfected on the full stack, but has been successfully performed on a shorter (9-layer) stack as shown in the SEM images in Fig. 10. While in Fig. 9(a) the waveguide is obscured, in Fig. 10(a) the waveguide is clearly observed after the thin rods have been removed.

While the rod periodicity *a* is not affected, the oxidation and etching process reduce the width and height of the main lattice rods, by about 150 nm in both dimensions leaving $w = 250$ nm and $h = 350$ nm (Fig. 10(a)). Similar final dimensions are expected on the 17-layer structures after the thin rods removal. Another issue is that the oxidation and etching process was not able to completely remove the thin rods throughout the structure, leaving very thin silicon wires of about 30 nm thickness. These thin wires can be seen in Fig. 10(a), for example at the topmost layer of the 9-layer structure. These residues have been incorporated in eigenmode simulations, and the conclusion is that as long as they are at least on unit cell distance (*a*) away from the woodpile waveguide wall, the accelerating mode is not affected.

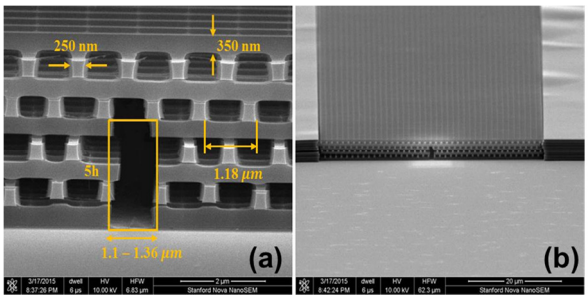

Figure 10. A 9-layer woodpile waveguide structure, after the removal of the supporting thin rods by oxidation and vapor HF etching.

The bandgap of the completed 9-layer structure was characterized by Fourier transform infrared spectroscopy. The normal incidence (perpendicular to the stacking direction) reflectance of the woodpile sample is measured, and compared with a finite-difference-time-domain (FDTD) simulation in Fig. 11. A distinct reflection peak with maximum reflectance close to 100% can be seen, with a full width at half maximum bandwidth from 2.4 to 3.9 μm, in close correspondence with the simulation (2.35 – 3.82 μm). The agreement of the bandgap center wavelength between measurement and simulation is within 3.2%. Narrow resonance features at the short wavelengths end of the simulation are observed, and show disagreement with the measurement near 2 um. While the accuracy of the simulation at shorter wavelengths could be further improved by using better absorption boundaries for higher frequencies as well as more refined mesh size, this discrepancy is also a true reflection of dimension differences between the fabricated sample and the modeled perfectly uniform structure, especially at high frequencies. Nevertheless, this bandgap characterization suggests an established fabrication process of woodpile waveguide structures with the required bandgap. Accelerator power coupler fabrication using the newly proposed dimensions is underway.

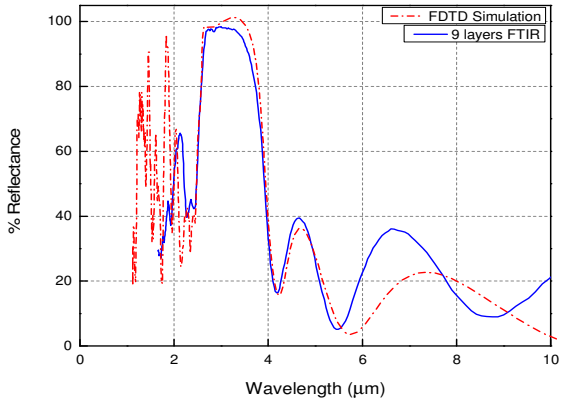

Figure 11. The reflectance spectra of a 9-layer woodpile structure. The measured data is in blue while the simulation is in red.

V. Discussion

A new accelerating mode in a silicon woodpile PBG structure has been proposed, with improved transverse profile, higher acceleration gradient, and larger group velocity. At the design wavelength near 1.55 μm, its Gaussian-like cross section mode area is increased by almost 100% from the previous accelerating mode design, resulting in better beam loading in terms of larger charge throughput and more efficient profile matching. Previously developed power coupler design methods for woodpile waveguides are applied, and over 75% total power transmission efficiency of laser power into this forward-propagating accelerating mode has been achieved via silicon side couplers. A fully forward coupler in its longitudinal dimension is designed, with cut-off sections preventing propagation of the accelerating mode outside the accelerator section. In simulations a good energy confinement and a high coupling efficiency of 76% are demonstrated. The lost 24% of the incident power mainly goes to the nonzero backward propagating wave ($|R| \sim 17.5\%$), as well as the power scattered into the woodpile lattice or back to the side couplers in a mode other than the excitation waveport mode. This spurious scattering of energy is clearly observed in the simulated model, as its electromagnetic fields plot exhibits strayed energy at both coupling corners of the structure, and signs of standing waves forming in the input and output side couplers.

In the coupler simulations, localized high field spots inside silicon at the coupling corner where silicon side guides insert into the accelerating waveguide are observed. These "hot spots" yields an acceleration factor of 0.18 for this forward coupler design, i.e., acceleration gradient inside the woodpile waveguide is 18% of the maximum magnitude of the electric fields inside silicon at these hot spots. Given this acceleration factor and taking into consideration the damage threshold fluence of ~ 0.35 J/cm^2 for silicon in vacuum near 1.506 μm [19], the maximum acceleration gradient that this fully forward coupler can be operated at is estimated to be about 185 MV/m, assuming a drive laser pulse of 1 picosecond duration.

This power coupler design is almost all-silicon, except the perfect conductor element embedded in the side coupler guide to launch a traveling wave (Fig. 5). Note that use of metals in the design makes the coupler structure prone to laser field damage, because of the much lower damage threshold of metals than dielectrics [19]. An air discontinuity in the silicon guide with carefully tuned dimensions, or one layer of other dielectric materials of high damage thresholds (e.g., silica and sapphire) [9, 20] might just as well fulfill the task of perturbing the side coupler guide. As already exposed in Fig. 9 and Fig. 10, dimension errors caused by fabrication and thermal drifts are expected in the manufactured structure. Previous attempt to study the fabrication error of the woodpile structure statistically, and deliberately overshoot the intended dimensions to compensate this error can be found in [21]. The same analysis could be applied to the membrane based stacking method in Section IV. It is challenging to quantitatively model thermal expansion of accelerator structures due to material absorption of laser power or electron beam heating. However, the collective effect of these errors in terms of the woodpile bandgap center frequency and the optimal coupling bands could be practically measured in its acceleration experiments. To compensate these deviations from design in real time, tuning mechanisms of the coupler are necessary during its operation. This may be achieved by micro heating elements [22, 23], liquid crystals [24], or MEMS devices on silicon [21, 25].

As presented in Section IV, woodpile accelerating waveguide structures up to 17 layers have been fabricated, with the targeted operating wavelength near 3 μm. The measured reflection bandgap is in direct agreement with the simulation, and the accelerating waveguide is made with dimensions close to the design. The inclusion of supporting thin rods has proven to be useful in strengthening the lattice rods and the whole structure in fabrication. Removal of these interstitial thin rods has been demonstrated in fabrication on 9-layer waveguide structures. New fabrications are ongoing, of a design with the new accelerating waveguide mode and no supporting rods in its vicinity as suggested by the accelerating mode simulation.

Acknowledgment

Fabrication of the 3D woodpile accelerators was conducted at Stanford Nanofabrication Facility and Stanford Nano Fabrication Center which is supported by U.S. Department of Energy through SLAC National Accelerator Laboratory under Grants DE-AC02-76SF00515 and DE-FG02-13ER41970, as well as by National Science Foundation through the NNIN under Grant ECS-9731293.

References

[1] T. Plettner P. P. Lu, and R. L. Byer, "Proposed few-optical cycle laser-driven particle accelerator structure," *Phys. Rev. ST Accel. Beams*, vol. 9, no. 11, pp. 111301- 111312, Nov. 2006.

[2] E. A. Peralta, K. Soong, R. J. England, E. R. Colby, Z. Wu, B. Montazeri, C. McGuiness, J. McNeur, K. J. Leedle, D. Walz, E. B. Sozer, B. Cowan, B. Schwartz, G. Travish, and R. L. Byer, "Demonstration of electron acceleration in a laser-driven dielectric microstructure," *Nature*, vol. 503, pp. 91-94, Nov. 2013.

[3] J. Breuer and P. Hommelhoff, "Laser-based acceleration of nonrelativistic electrons at a dielectric structure," *Phys. Rev. Lett.*, vol. 111, no. 13, pp. 134803-134807, Sept. 2013.

[4] K. J. Leedle, R. F. Pease, R. L. Byer, and J. S. Harris, "Laser acceleration and deflection of 96.3 keV electrons with a silicon dielectric structure," *Optica*, vol. 2, no. 2, pp. 158-161, Feb. 2015.

[5] X. Lin, "Photonic band gap fiber accelerator," *Phys. Rev. ST Accel. Beams*, vol. 4, no. 5, pp. 051301-051307, May 2001.

[6] B. M. Cowan, "Three-dimensional dielectric photonic crystal structures for laser-driven acceleration," *Phys. Rev. ST Accel. Beams*, vol. 11, no. 1, pp. 011301-011309, Jan. 2008.

[7] J. D. Joannopoulos, S. G. Johnson, J. N. Winn, and R. D. Meade, in *Photonic Crystals: Molding the Flow of Light*, 2nd ed., Princeton Univ. Press, Princeton, NJ.

[8] A. Mizrahi and L. Schachter, "Optical Bragg accelerators," *Phys. Rev. E*, vol. 70, no. 1, pp. 016505 1-21, Jul. 2004.

[9] Z. Wu, R. J. England, C. K. Ng, B. M. Cowan, C. McGuinness, C. H. Lee, M. H. Qi, and S. Tantawi, "Coupling power into accelerating mode of a three-dimensional silicon woodpile photonic band-gap waveguide," *Phys. Rev. ST Accel. Beams*, vol. 17, no. 8, pp. 081301-081313, Aug. 2014.

[10] C. K. Ng, R. J. England, L. Q. Lee, R. Noble, V. Rawat, and J. Spencer, "Transmission and radiation of an accelerating mode in a photonic band-gap fiber," *Phys. Rev. ST Accel. Beams*, vol. 13, no. 12, pp. 121301-121310, Dec. 2010.

[11] Z. Wu, "Dipole modes in a silicon woodpile structure for sub-micron beam position monitoring," unpublished.

[12] B. M. Cowan, "Photonic crystal laser-driven accelerator structures," Ph.D. dissertation, Appl. Phys. Dept., Stanford Univ., Stanford, CA, 2007.
[13] C. Nantista, S. Tantawi, and V. Dolgashev, "Low-field accelerator structure couplers and design techniques," *Phys. Rev. ST Accel. Beams*, vol. 7, pp. 072001 1-7, Jul. 2004.
[14] N. M. Kroll, C.-K. Ng, and D. C. Vier, "Applications of time domain simulation to coupler design for periodic structures," SLAC-PUB-8614, Sept. 2000.
[15] High Frequency Structure Simulator, version 13, ANSYS Corporation.
[16] C. McGuinness, E. Colby, and R. L. Byer, "Accelerating electrons with lasers and photonic crystals," *J. Mod. Opt.*, vol. 56, pp. 2142-2147, Sept. 2009.
[17] I. Staude, C. McGuinness, A. Frolich, R. L. Byer, E. Colby, and M. Wegener, "Waveguides in three-dimensional photonic bandgap materials for particle-accelerator on a chip architectures," *Opt. Express*, vol. 20, no. 5, pp. 5607-5612, Feb. 2012.
[18] M. A. Hartney, D. W. Hess, and D. S. Soane, "Oxygen plasma etching for resist stripping and multilayer lithography," *J. Vac. Sci. Technol. B*, vol. 7, pp. 1-13, Feb. 1989.
[19] K. Soong, R.L. Byer, C. McGuinness, E. Peralta, and E. Colby, "Experimental determination of damage threshold characteristics of IR compatible optical materials," SLAC-PUB-14415, May 2011.
[20] H. T. Chen and K. J. Webb, "Silicon-on-insulator irregular waveguide mode converters," *Opt. Lett.*, vol. 31, no. 14, pp. 2145-2147, Jul. 2006.
[21] C. McGuinness, E. Colby, B. Cowan, R.J. England, J. Ng, R.J. Noble, E. Peralta, K. Soong, J. Spencer, D. Walz, and R.L. Byer, "Fabrication and characterization of woodpile structures for direct laser acceleration," *AIP Conf. Proc.*, vol. 1299, pp. 439-444, Jun. 2010.
[22] R. Soref, "The past, present, and future of silicon photonics," *IEEE J. Sel. Top. Quantum Electron.*, vol. 12, no. 6, pp. 1678-1687, Nov. 2006.
[23] M. W. Pruessner, T. H. Stievater, M. S. Ferraro, and W. S. Rabinovich, "Thermo-optic tuning and switching in SOI waveguide Fabry-Perot microcavities," *Opt. Express*, vol. 15, no. 12, pp. 7557-7563, Jun. 2007.
[24] J. Cos., J. Ferré-Borrull, J. Pallarès, and L. F. Marsal, "Optimal tunability of waveguides based on silicon photonic crystals infiltrated with liquid crystals," *Opt. Quant. Electron.*, vol. 42, pp. 487-497, Jan. 2011.
[25] A. Lipson, "A tunable micro-electro-mechanical optical filter in silicon," Ph.D. dissertation, Dept. Electric. Electron. Eng,. Imperial College London, London, United Kingdom, 2006.

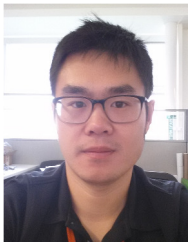

Ziran Wu was born in Hefei, China in 1982. He received his B.Sc. degree in physics from the University of Science and Technology of China, Hefei in 2004, and both his Ph.D. degree in physics and M.Sc. degree in electrical and computer engineering from the University of Arizona, Tucson in 2010. Since August 2010, he has been working in the SLAC National Accelerator Laboratory at Menlo Park, California, first as a Research Associate and then a Staff Scientist. His research interests include photonic crystal based components, devices, and technology, ultrafast science, terahertz radiation sources, and THz nano-materials characterization. His current work is focused on micro-accelerators using ultrafast laser and photonic structures, and accelerator based THz sources and experiments.

Chunghun Lee was born in Gangneung, South Korea, in 1980. He received the B.S. degrees in electronic engineering from the Gangneung National Universiy, Gangneung, South Korea, in 2006 and the Ph.D. degree in electrical and computer engineering from Purdue University, West Lafayette, IN, in 2015.

From 2012 to 2014, he was a visiting scientist at SLAC National Accelerator Laboratory. Since 2015, he has been a project scientist at SLAC. His research interests include nano-scale fabrication, precise alignment stage setup, three dimensional photonic crystals, and laser accelerators with dielectric materials.

Kent P. Wootton was born in 1985. He was awarded the degrees BSc (Hons) with majors in physics and mathematics, and the degree of BE (Hons) in civil engineering from Monash University, Clayton, Victoria, Australia in 2010, and the PhD in physics from The University of Melbourne, Parkville, Victoria, Australia in 2014.

Since 2014, he has worked as an Experimental Research Associate at SLAC National Accelerator Laboratory, Menlo Park, California, USA. His research interests in electron accelerators include dielectric laser accelerators, ultralow vertical emittance beams, spin-polarized beams, and beam diagnostics based on synchrotron light and undulator radiation.

Dr. Wootton is a member of the Australian Institute of Physics and the American Physical Society.

Cho-Kuen Ng obtained his Ph. D. in High Energy Physics from the University of Illinois at Urbana-Champaign in 1986. After postdoctoral work in particle phenomenology at the University of Durham, England and in computational plasma physics at Cornell University, he has been with the SLAC National Accelerator Laboratory since 1991. Dr. Ng's research focuses on electromagnetic simulations of particle accelerators, in particular in the area of wakefield computations of accelerator cavities and beamline components using high performance computing. He has contributed to many accelerator projects including the design and analysis of the PEP-II, NLC, ILC, SPEAR3, LCLS and dielectric laser acceleration at SLAC. Currently, Dr. Ng is the institutional PI of the US DOE SciDAC ComPASS accelerator project and is leading a multi-disciplinary team of physicists and computational scientists in developing parallel multi-physics finite-element electromagnetic codes for large-scale accelerator applications.

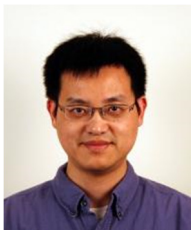

Minghao Qi (M'05) was born in Jiangsu, China in 1973. He received the B.S. in Chemical Physics from the University of Science and Technology of China, Anhui, China, in 1995 and the Ph.D. degree in Electrical Engineering and Computer Science from Massachusetts Institute of Technology, Cambridge, MA, in 2005.

In 2005 he joined the School of Electrical and Computer Engineering of Purdue University as an Assistant Professor,

and has become an Associate Professor since 2011. He is the author of more than 50 articles and over 120 conference papers. His research interests include the design, fabrication, and characterization of silicon-on-insulator photonic devices, development of new lithographic techniques for integrated-circuit patterns, and low-cost manufacturing of silicon solar cells. He received a young investigator award from the Defense Threat Reduction Agency in 2010.

R. Joel England obtained his PhD in accelerator physics at the University of California Los Angeles, where he developed a method of generating tailored drive beams for more efficient excitation of plasma-based particle accelerators and designed a novel low-power X-band deflecting mode cavity for use as a particle beam temporal diagnostic. In parallel with his graduate studies, he did consulting work on X-band cavity design and on magnetostatic design. In 2008, Dr. England joined the Advanced Accelerator Research Department at SLAC, led by Dr. Eric Colby and Prof. Bob Siemann, as a postdoctoral researcher working on optical-scale particle accelerators powered by solid state lasers. Dr. England is currently a Panofsky Fellow at SLAC and leader of the Dielectric Laser Acceleration Group, which, in collaboration with the research group of Prof. Robert Byer at Stanford, has recently developed and performed the first demonstrations of high-gradient acceleration in laser-driven dielectric structures. Dr. England has served as a working group co-leader for the Advanced Accelerator Concepts Workshop and the APS DPF Meeting, a grant reviewer for the National Science Foundation and the Department of Energy, and on various organizational committees. He is author or co-author on over 50 publications and proceedings, and has given talks at numerous particle accelerator conferences and workshops.